

# Double jumps for two dipole-interacting atoms

Sören Addicks<sup>1</sup>, Almut Beige<sup>2</sup>, Mohammed Dakna<sup>1</sup> and Gerhard C. Hegerfeldt<sup>1</sup>

<sup>1</sup>*Institut für Theoretische Physik, Universität Göttingen,  
Bunsenstr. 9, 37073 Göttingen, Germany*

<sup>2</sup>*Optics Section, Blackett Laboratory, Imperial College London,  
London SW7 2BZ, England*

(December 2, 2024)

Cooperative effects in the fluorescence of two dipole-interacting atoms, with macroscopic quantum jumps (light and dark periods), are investigated. We present, to our knowledge for the first time, theoretical results which predict cooperative effects for double jumps between periods of double intensity and dark periods for atomic distances from one and to ten wave lengths of the strong transition. The double jump rate, as a function of the atomic distance, can show oscillations of up to 30% at distances of about a wave length. Cooperative effects are still noticeable at a distance of ten wave lengths. The results are obtained both by simulations and analytically. The transition rates between different intensity periods are calculated in closed form and are used to determine the double jump rates, the mean duration of the three intensity periods and the mean rate of their occurrence. These quantities are shown to exhibit cooperative effects and their characteristic behavior turns out to be strongly dependent on the laser detuning.

42.50.Ar, 42.50.Fx

## I. INTRODUCTION

The dipole-dipole interaction between two atoms can be understood through the exchange of virtual photons and depends on the transition dipole moment of the levels involved. It can be characterized by complex coupling constants whose real part affects decay constants and whose imaginary part leads to level shifts [1]. The coupling constants drop off in an oscillatory way as  $1/r$  for atomic distances larger than about a wave length of the transition. Cooperative effects in the radiative behavior of atoms which may arise from their mutual dipole-dipole interaction have attracted considerable interest in the literature [1]- [28]. Recently, a system of two two-level atoms at a distance much less than a wave length was considered as a quantum information channel and the role of the dipole interaction was studied [29]. Two of the present authors [30] have investigated in detail the transition from anti-bunching to bunching with decreasing atomic distance for two dipole-dipole interacting two-level atoms. The relevance for decoherence processes in the realization of quantum logic gates in ion traps has been pointed out in Ref. [31].

The striking phenomenon of macroscopic quantum jumps (electron shelving or macroscopic dark and light periods) can occur for a multi-level system where the electron is essentially shelved for seconds or even minutes in a metastable state without photon emissions [32]- [41]. For two such systems the fluorescence behavior would, without cooperative effects, be just the sum of the separate photon emissions, with dark periods of both atoms, light periods of a single atom and of two atoms. In Ref. [42] the fluorescence intensity of three such ions in a Paul trap was measured and a large fraction of almost simultaneous jumps by two and even all three ions was recorded.

This fraction was orders of magnitudes larger than that expected for independent ions. A quantitative explanation of such a large cooperative effect for distances of the order of ten wave lengths of the strong transition has been found to be difficult [13,43-46]. Other experiments at larger distances and with different ions showed no cooperative effects [47,48].

Quite recently, two of the present authors [49] investigated cooperative effects in the mean duration,  $T_0$ ,  $T_1$ , and  $T_2$ , of the three different types of fluorescence periods, i.e. dark, single-intensity, and double-intensity periods, respectively. This was done by simulations for two atoms in a  $V$  configuration. The mean duration of the single- and double-intensity periods,  $T_1$  and  $T_2$ , depended sensitively on the dipole-dipole interaction and thus on the atomic distance  $r$ . They exhibited noticeable oscillations which decreased in amplitude when  $r$  increased. These oscillations seemed to continue up to a distance of well over five wave lengths of the strong transition and they were *opposite* in phase with those of  $\text{Re } C_3(r)$ , where  $C_3$  is the complex dipole-dipole coupling constant associated with the strong transitions.

In this paper we present, to our knowledge for the first time, theoretical results which predict cooperative effects in the double jumps of two dipole-dipole interacting atoms. These results are for atoms in the  $V$  configuration (see Fig. 1), obtained both by simulations and explicitly in closed analytic form.

The simulations of double jump rates are performed for atomic distances from three quarters of a wave length of the strong transition to ten wave lengths and for zero laser detuning. As a function of the atomic distance, the simulated double jump rates show marked oscillations, with a maximal difference of up to 30%, decreasing as  $1/r$  and *in phase* with  $\text{Re } C_3(r)$ . These simulations re-

quire extremely long trajectories of photon emissions and can therefore only be performed for suitable parameters, i.e. decay constants, Rabi frequencies and laser detunings. The immediate question arises how to compare with possible experiments and how universal the resulting conclusions are. For example, can the oscillation amplitude be much larger if the parameters are changed or, for that matter, much smaller? Or, is the variation always in phase with  $\text{Re } C_3(r)$ ? To answer these questions an analytic treatment is needed, which will not only cover other, experimentally interesting, parameters but will also provide a better understanding.

Therefore, in a tour de force, we first calculate, in closed form, the transition probability rates between the three different types of fluorescence periods for two atoms in a  $V$  configuration, at a fixed distance  $r$  and for general values of the strong decay constant, Rabi frequencies and detuning of the laser driving the weak atomic transition. With these transition probability rates all relevant quantities like double jump rates and mean duration of the three types of fluorescence periods are obtained explicitly.

The analytic results for double jump rates are compared with the simulations, taking into account the data-smoothing procedure employed in the simulations. The agreement is excellent. This is also true for new simulations of the mean duration of the fluorescence periods which are presented in this paper. However, for parameters different from those used in the simulations the analytic results contain unexpected and surprising features. The most surprising is a change in the oscillatory behavior of the double jump rate from *in phase* with  $\text{Re } C_3(r)$  to *opposite* in phase when the detuning of the laser driving the weak atomic transition is increased. For the mean durations  $T_1$  and  $T_2$  there can be a change in behavior from opposite in phase to *in phase* with  $\text{Re } C_3(r)$ . Moreover, for a particular value of the detuning, which depends on the other parameters, the double jump rate becomes *constant* in  $r$  and the cooperative effects disappear. This is true also for the mean period durations and for their mean occurrences, with a different value of the detuning, though. Typically, for nonzero detuning the oscillation amplitudes do not exceed those found for zero detuning.

The experiments of Ref. [42] exhibited extremely large cooperative effects, in fact up to three orders of magnitude. One should bear in mind, however, that this was for a different atomic level configuration and for *three* ions in a trap. In principle our analytic approach can be carried over to the experimental situation of Ref. [42], but the calculations become algebraically even more involved and have not been carried out here.

The plan of the paper is as follows. In Section II we present the simulation results for double jumps. In Section III we collect the prerequisites of our analytic approach. The Bloch equations for two  $V$  systems, which are irradiated by two lasers, are given and it is indicated how the dipole-dipole interaction arises. In Section IV

the fluorescence with its three different intensity periods is treated as a three-step telegraph process and the transition probability rates between the three periods are derived by means of a resolvent expansion and the Bloch equations. This is the most difficult and complex part of the paper. In Section V an expression for the double jump rate is obtained in terms of these transition rates. The result is compared with the simulation and its dependence on the detuning is studied. In Section VI the mean duration of the three types of fluorescence periods are determined in terms of the transition rates. The expressions are compared with a new simulation and their dependence on the detuning is investigated. In the last section the results are discussed. It is suggested that the mean rate of double-intensity periods is an experimentally easily accessible candidate for exhibiting cooperative effects arising from the dipole-dipole interaction.

## II. SIMULATION OF DOUBLE JUMPS

Dark periods in the fluorescence of a single atom occur in the case of a  $V$  configuration with a metastable state because of two widely different time scales in the times between two subsequent photon emissions (cf., e.g. Refs. [38,41,50–52]). The small time scale is of the order of  $A_3^{-1}$  or  $\Omega_3^{-1}$  and the larger is of the order of  $\Omega_3/\Omega_2^2$ , where  $A_3$  is the Einstein coefficient of the strong transition and the  $\Omega_i$  are Rabi frequencies (see Fig. 1).

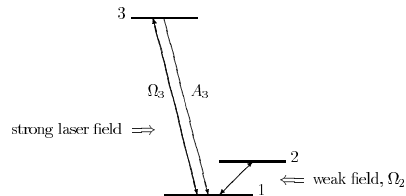


FIG. 1.  $V$  system with metastable level 2 and Einstein coefficient  $A_3$  for level 3.  $\Omega_2$  and  $\Omega_3$  are the Rabi frequencies of the two lasers driving the weak 1-2 transition and the strong 1-3 transition, respectively.

Picking an intermediate time  $\tilde{T}$  one can define a light period as a sequence of photon emissions with waiting times less than  $\tilde{T}$ . A waiting time longer than  $\tilde{T}$  corresponds to a dark period. One can usually take  $\tilde{T}$  around  $10 A_3^{-1}$ . Since the average duration of a light and a dark period is in general much longer than  $\tilde{T}$  these periods are very precisely defined. By means of the quantum jump approach [50–54] it can be shown that the occurrence of the fluorescence periods can be described, to high precision, as a telegraph process [55,56].

For two *independent*, noninteracting, atoms the photon emission sequence is just the sum of the individual contributions. The different periods overlap and give rise to fluorescence periods of zero, single and double intensity, denoted as periods of type 0, 1 and 2, respectively. These are describable as a three-step telegraph process.

Since the periods differ only by the *average* number of photons per unit time, the identification of single and double intensity periods is observationally more difficult if one does not record from which atom the individual photons came. Due to fluctuations, the transitions are then not so sharply defined any longer. This is illustrated in Fig. 2 which shows part of a typical photon sequence.



FIG. 2. Part of a simulated photon sequence. Each vertical line denotes an emission.

The same problem arises for two atoms which are sufficiently close and *dipole interacting*. To distinguish different periods one has to use the average photon intensity, obtained e.g. by means of averaging over a time window. This window has to be large enough to contain enough emissions, but must not be too large in order not to overlook too many short periods. For the averaging we have used a moving window [57] of fixed width, denoted by  $\Delta T_w$ . Fig. 3 shows part of a resulting intensity curve for  $\Delta T_w = 114 A_3^{-1}$ . A similar averaging procedure is also present in experiments.

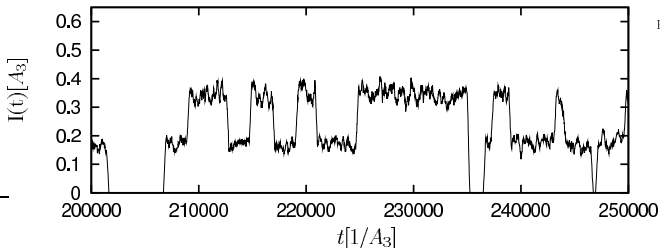


FIG. 3. Intensity obtained by averaging with a moving window. At  $t = 235000 A_3^{-1}$  there is a double jump.

A double jump is defined as a transition from a double-intensity period to dark period, or vice versa, within a prescribed time interval  $\Delta T_{DJ}$ . This interval should be larger than  $\Delta T_w$ . Here we have chosen  $\Delta T_{DJ} = 684 A_3^{-1}$ . Fig. 3 shows such a double jump at  $t = 235000 A_3^{-1}$ . In view of intensity fluctuations it has turned out as reasonable for the simulation algorithm to record a double jump whenever the intensity difference within  $\Delta T_{DJ}$  is at least 90 % of the mean intensity of periods of type 2. Since double jumps are rare events, long simulation paths are needed. In our case their lengths were  $10^8 A_3^{-1}$ , corresponding to  $1.7 \times 10^7$  photons for the parameters used here.

Paths of photon emissions have been produced by the same simulation technique as in Ref. [49]. It has been assumed that the lasers are perpendicular to the line connecting the atoms and that the dipole moments are parallel. Definite numerical values of the parameters are taken for the simulations, satisfying

$$\Omega_2 \ll \Omega_3, \quad \Omega_2 \ll \Omega_3^2/A_3, \quad A_2 \approx 0, \quad (1)$$

with *zero* laser detunings. For such parameters an individual atom exhibits macroscopic light and dark periods. From a given simulation path we have determined the double jump rate. First of all the simulated rates for upward and downward double jumps have been found to be equal in the simulations. Then we have studied the double jump rate for various atomic distances. The  $r$  dependence of the rate depended somewhat on the chosen averaging window  $T_w$ . This is illustrated in Figs. 4 (a) and (b).

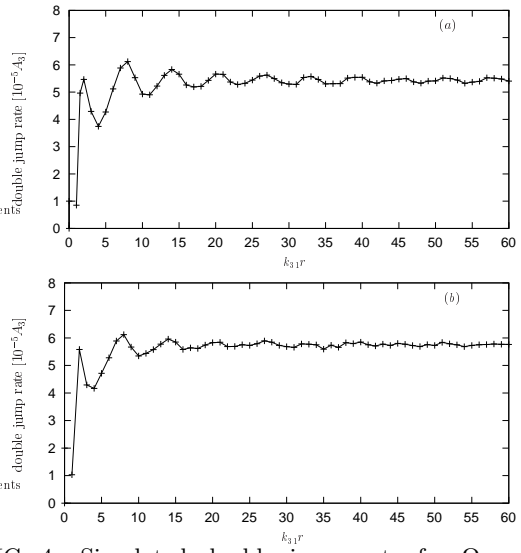


FIG. 4. Simulated double jump rate for  $\Omega_3 = 0.5 A_3$ ,  $\Omega_2 = 0.01 A_3$ ,  $T_{DJ} = 684 A_3^{-1}$  and zero detuning. Averaging windows (a)  $T_w = 114 A_3^{-1}$ , (b)  $T_w = 174 A_3^{-1}$ . For larger averaging window the features are washed out.

In both figures we have chosen  $\Omega_3 = 0.5 A_3$  and  $\Omega_2 = 0.01 A_3$ , but for the former we have taken  $\Delta T_w = 114 A_3^{-1}$  and for the latter  $\Delta T_w = 174 A_3^{-1}$ . Fig. 4 (a) shows distinct features which are somewhat washed out in Fig. 4 (b) with the larger  $\Delta T_w$ . A larger  $\Delta T_w$  gives a smoother intensity curve, but makes the determination of the transition times between different periods more difficult, while a shorter averaging window introduces more noise. We found the use of  $\Delta T_w = 114 A_3^{-1}$  to be a good compromise.

In Fig. 4 (a) the double jump rate exhibits marked oscillations with the atomic distance  $r$  for  $5 \leq k_{31}r \leq 40$ , where  $k_{31} = \omega_{31}/c$  is the wave number for the 3-1 transition. Around  $k_{31}r = 2\pi$ , i.e. for atomic distances of about a wavelength of the strong transition, the double jump rate changes by up to 30%. For  $k_{31}r < 5$ , i.e. for atomic distances smaller than three quarters of a wavelength of the strong transition, the total emission intensity decreases, due to the level shifts caused by the dipole interaction (cf. the imaginary part of  $C_3$  in Eq. (9) below). Furthermore, periods of type 2 and 1 are no longer easily discernible since the intensity ratio decreases.

Comparison with  $C_3$  in Fig. 5 below shows that the simulated double jump rate oscillates with  $r$  *in phase*

with  $\text{Re } C_3$ . When  $\text{Re } C_3$  increases the double jump rate decreases, and vice versa. The oscillation amplitude decreases with  $r$ , just as  $\text{Re } C_3$  does. On the other hand  $\text{Im } C_3$ , which is shifted by about  $\pi$  with respect to  $\text{Re } C_3$ , does not seem to play any role for the results of the simulations.

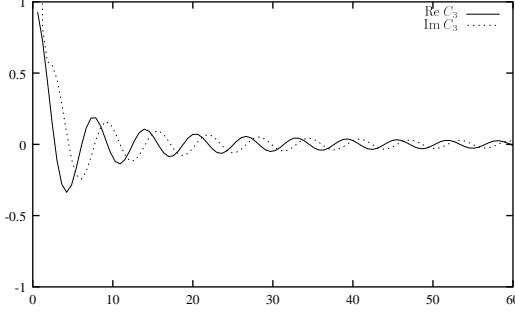


FIG. 5. The complex dipole-dipole coupling constant  $C_3$  for the strong transition as a function of the atomic distance.

The question which arises immediately is whether this behavior is typical or an artifact of the special choice of parameters. In order to study this we will determine the double jump rate analytically and compare the results with the simulation results. It will be shown that for atomic distances greater than three quarters of a wave length of the strong transition (i) the upward and downward double jump rates are indeed equal; (ii) for small detuning,  $\Delta_2$ , of the weak driving the double jump rate does vary in phase with  $\text{Re } C_3(r)$ , but for larger  $\Delta_2$  there is an unexpected change to a behavior opposite in phase; (iii) the oscillations do not exceed 30%; (iv) for a particular choice of  $\Delta_2$  the double jump rate can become practically constant, i.e. independent of  $r$ .

### III. THE BLOCH EQUATIONS

In this section we will present the prerequisites necessary for the analytic treatment of the transition probabilities between the three intensity periods. We consider two atoms, each a  $V$  configuration as shown in Fig. 1, with the levels  $|1\rangle_i$ ,  $|2\rangle_i$  and  $|3\rangle_i$  ( $i = 1, 2$ ) and fixed at positions  $\mathbf{r}_i$ . For the  $i$ -th atom, we define raising and lowering operators  $S_{ij}^\pm$  ( $j = 2, 3$ ) by  $S_{ij}^+ = |j\rangle_{ii}\langle 1|$  and  $S_{ij}^- = |1\rangle_{ii}\langle j|$ . For simplicity we consider the case where the dipole moments of the atoms are the same, i.e.  ${}_1\langle 1|\mathbf{X}_1|j\rangle_1 = {}_2\langle 1|\mathbf{X}_2|j\rangle_2 \equiv \mathbf{D}_{1j}$ . If  $\mathbf{D}_{1j}$  is real we can denote the angle it forms with the line connecting the atoms by  $\vartheta_j$ . In general,  $\vartheta_j$  is defined through  $\cos^2 \vartheta_j = |(\mathbf{D}_{1j}, \mathbf{r})|^2 / r^2 D_{1j}^2$ , where  $\mathbf{r} = \mathbf{r}_2 - \mathbf{r}_1$ . We assume the laser radiation normal to this line so that the lasers are in phase for both atoms. The two lasers are denoted by  $L_2$  and  $L_3$  and their electric field by  $\mathbf{E}_{Lj}(\mathbf{r}, t) = \text{Re}[\mathbf{E}_{0j} \exp\{-i(\tilde{\omega}_j t - \mathbf{k} \cdot \mathbf{r})\}]$ . The detuning is  $\Delta_j = \tilde{\omega}_j - \omega_{j1}$  where  $\hbar\omega_{j1}$  is the energy difference be-

tween level 1 and level  $j$ . In the following we choose zero detuning for the strong laser. Making the usual rotating-wave approximation and going over to the appropriate interaction picture the interaction Hamiltonian becomes

$$H_I = - \sum_{i=1}^2 \hbar \Delta_2 S_{i2}^+ S_{i2}^- + \sum_{i=1}^2 \sum_{j=2}^3 \sum_{\mathbf{k}, s} \hbar [g_{j \mathbf{k}, s} a_{\mathbf{k}, s} e^{i(\tilde{\omega}_j - \omega_k)t} e^{i\mathbf{k} \cdot \mathbf{r}_i} S_{ij}^+ + \text{H.c.}] + H_L , \quad (2)$$

with the coupling constants

$$g_{j \mathbf{k}, s} = ie \left( \frac{\omega_k}{2\epsilon_0 \hbar L^3} \right)^{1/2} (\mathbf{D}_{1j}, \epsilon_{\mathbf{k}, s}) , \quad (3)$$

and laser part

$$H_L = \frac{\hbar}{2} \sum_{i=1}^2 \sum_{j=2}^3 \Omega_j \{ S_{ij}^+ + S_{ij}^- \} . \quad (4)$$

The Rabi frequency of the laser driving the  $1-j$  transition is  $\Omega_j = (e/\hbar) \mathbf{D}_{1j} \cdot \mathbf{E}_{0j}$ . It is the same for both atoms and can be assumed real. The operator  $H_I$  implicitly contains the dipole-dipole interaction of the two atoms, as seen from the conditional Hamiltonian  $H_{\text{cond}}$  further below. In the Power-Zienau formulation, which we have used above, this interaction is due to photon exchange [1]. For the Einstein coefficients, the Rabi frequencies and the detuning we assume the relations

$$\Omega_2 \ll \Omega_3 , \quad \Omega_2 \ll \Omega_3^2/A_3 , \quad A_2 \approx 0 , \quad \Delta_3 = 0 , \quad \Delta_2 \text{ arbitrary.} \quad (5)$$

which, except for the more general detuning, is the same as in Eq. (1).

From the above Hamiltonian one obtains, as in Ref. [49], the conditional Hamiltonian  $H_{\text{cond}}$  of the quantum jump approach [50–54], which describes the time development between photon emissions, and the reset operation  $\mathcal{R}$ , which determines the (non-normalized) state  $\mathcal{R}(\rho)$  right after a photon emission. As shown in Refs. [30,52] the Bloch equations can be written in the compact form

$$\dot{\rho} = - \frac{i}{\hbar} [H_{\text{cond}}\rho - \rho H_{\text{cond}}^\dagger] + \mathcal{R}(\rho) . \quad (6)$$

$\mathcal{R}$  and, except for the detuning, also  $H_{\text{cond}}$  are given by the same expressions as in Ref. [49].

Again it is convenient to introduce Dicke states. Let  $|g\rangle$ ,  $|e_2\rangle$  and  $|e_3\rangle$  denote the states where both atoms are in the ground state and in the excited states  $|2\rangle$  and  $|3\rangle$ , respectively, and let  $|s_{jk}\rangle$  be the symmetric and  $i|a_{jk}\rangle$  be the antisymmetric combinations of  $|j\rangle|k\rangle$  and  $|k\rangle|j\rangle$ . Then the reset operation is as in Ref. [49],

$$\mathcal{R}(\rho) = (A_3 + \text{Re } C_3) R_+ \rho R_+^\dagger + (A_3 - \text{Re } C_3) R_- \rho R_-^\dagger \quad (7)$$

where

$$\begin{aligned} R_+ &= (S_{13}^- + S_{23}^-) / \sqrt{2} \\ &= |g\rangle\langle s_{13}| + |s_{13}\rangle\langle e_3| + (|s_{12}\rangle\langle s_{23}| - |a_{12}\rangle\langle a_{23}|) / \sqrt{2}, \end{aligned}$$

$$\begin{aligned} R_- &= (S_{13}^- - S_{23}^-) / \sqrt{2} \\ &= |g\rangle\langle a_{13}| + |a_{13}\rangle\langle e_3| + (|s_{12}\rangle\langle a_{23}| + |a_{12}\rangle\langle s_{23}|) / \sqrt{2}. \end{aligned} \quad (8)$$

The conditional Hamiltonian is given by

$$\begin{aligned} H_{\text{cond}} &= -\hbar\Delta_2 [2|e_2\rangle\langle e_2| + |s_{12}\rangle\langle s_{12}| + |a_{12}\rangle\langle a_{12}| + |s_{23}\rangle\langle s_{23}| + |a_{23}\rangle\langle a_{23}|] \\ &+ \frac{\hbar}{2i} \left[ A_3 (|s_{23}\rangle\langle s_{23}| + |a_{23}\rangle\langle a_{23}|) + (A_3 + C_3)|s_{13}\rangle\langle s_{13}| + (A_3 - C_3)|a_{13}\rangle\langle a_{13}| + 2A_3|e_3\rangle\langle e_3| \right. \\ &\left. + \left\{ \sum_{j=2}^3 \sqrt{2}i\Omega_j (|g\rangle\langle s_{1j}| + |s_{1j}\rangle\langle e_j|) + i\Omega_2 (|s_{13}\rangle\langle s_{23}| + |a_{13}\rangle\langle a_{23}|) + i\Omega_3 (|s_{12}\rangle\langle s_{23}| - |a_{12}\rangle\langle a_{23}|) + \text{H.c.} \right\} \right] \end{aligned} \quad (9)$$

where  $r$ -dependent dipole-dipole coupling constants  $C_j$  are defined as

$$\begin{aligned} C_j &= \frac{3A_j}{2} e^{ik_{j1}r} \left[ \frac{1}{ik_{j1}r} (1 - \cos^2 \vartheta_j) \right. \\ &\left. + \left( \frac{1}{(k_{j1}r)^2} - \frac{1}{i(k_{j1}r)^3} \right) (1 - 3\cos^2 \vartheta_j) \right]. \end{aligned} \quad (10)$$

For  $A_2 \approx 0$  one has  $C_2 \approx 0$ . Thus one can neglect the dipole interaction when one atom is in state  $|2\rangle$ . The dependence of  $C_3$  on  $r$  is maximal for  $\vartheta_3 = \pi/2$  and the corresponding  $C_3$  is plotted in Fig. 5. For atomic distances greater than about three quarters of a wave length of the strong transition,  $|C_3|$  is less than  $0.2 A_3$ , but for smaller distances  $\text{Re } C_3$  approaches  $A_3$  and  $\text{Im } C_3$  diverges. From Eq. (9) one sees that  $\text{Re } C_3$  changes the spontaneous decay rates and that  $\text{Im } C_3$  leads to level shifts. Therefore, for small  $r$ , the decay rate of  $|a_{13}\rangle$  approaches 0 in this case and the large level shifts cause a decrease of fluorescence associated with the levels  $|s_{13}\rangle$  and  $|a_{13}\rangle$ .

Without lasers the conditional Hamiltonian is diagonal in the Dicke basis. In Fig. 6 the Dicke states and the possible transitions are displayed.

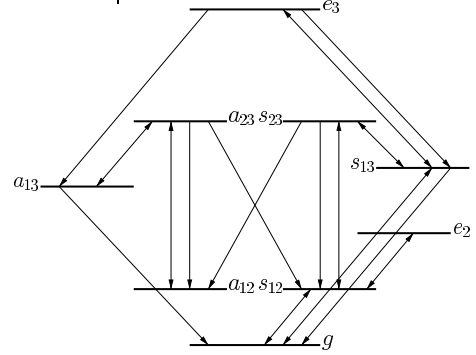


FIG. 6. Dicke states. The dashed and solid double arrows denote weak and strong driving, respectively. Simple arrows denote decays.

Dashed double arrows indicate the weak driving by laser 2, solid double and single arrows indicate strong driving by laser 3 and decay, respectively. For  $\Omega_2 = 0$ , i.e. with the dashed arrows absent, the states decompose into three non-connected subspaces, namely one spanned by  $|e_2\rangle$  and the two others spanned by the four states of the inner ring and outer ring in Fig. 6:

$$\begin{aligned} \text{dark state (type 0)} &: |e_2\rangle \\ \text{inner states (type 1)} &: |s_{12}\rangle, |a_{12}\rangle, |s_{23}\rangle, |a_{23}\rangle \\ \text{outer states (type 2)} &: |g\rangle, |s_{13}\rangle, |a_{13}\rangle, |e_3\rangle \end{aligned} \quad (11)$$

As in Ref. [49] we associate these subspaces with the fluorescence periods of type 0, 1, and 2, respectively. The weak laser will lead to slow transitions between these states.

#### IV. ANALYTIC DETERMINATION OF TRANSITION RATES

For the appearance of macroscopic light and dark periods of a *single* atom the existence of two different *time*

scales are of utmost importance [38]. The quantum jump approach [50–54] can be used to directly analyze the stochastic sequence of individual photon emission. It yields a telegraph process with light and dark periods and gives expressions for the transition probabilities between the periods. The quantum jump approach is also a very useful tool for the simulation of single trajectories.

If the times of the individual photon emissions are not known the state of the system has to be described by a density matrix. In a short time  $\delta t$  of the order of about  $5 A_3^{-1}$  after the beginning of a light period the atom rapidly approaches the equilibrium state corresponding to  $\Omega_2 = 0$  in the 1-3 subspace, as shown in Refs. [55,56]. Thereafter, on a longer time scale — much longer than  $A_3^{-1}$ , but much shorter than  $\Omega_2^{-1}$  — the driving by  $\Omega_2$  slowly builds up a small population in the metastable state  $|2\rangle$ , and this gives a small transition probability to the dark period. During the latter the atom is overwhelmingly in the metastable state, but it has a small component in the 1-3 subspace. This component in turn determines the transition probability to a light period. A more heuristic derivation of the transition probabilities starts from the intuitive assumption of a telegraph process and the overwhelming occupation of the subspaces spanned by  $|1\rangle$  and  $|3\rangle$  and by  $|2\rangle$ , respectively [37]. One can then use the Bloch equations to calculate the build-up during a time  $\Delta t$  of a population outside the respective subspace and to obtain from this the probability of leaving the subspace during  $\Delta t$ . This probability is then interpreted as the transition probability from one period to the other. The results agree with those of the more microscopic quantum jump approach.

A similar idea will be used here for *two* dipole-interacting  $V$  systems. We associate each of the three types of fluorescence periods with one of the subspaces spanned by the states in Eq. (11). At the beginning of a period of type 0, 1, or 2, the state of the two atoms is assumed to lie in the corresponding subspace. As before, in a short time  $\delta t$ , of the order of about  $5 A_3^{-1}$ , the state will approach the equilibrium state in this subspace corresponding to  $\Omega_2 = 0$ , since during this short time the driving by  $\Omega_2$  is negligible. We denote this equilibrium state by  $\rho_{ss,i}^{C_3}$ ,  $i = 0, 1, 2$ . Then, until a time  $\Delta t$ , satisfying

$$\Omega_3^{-1}, A_3^{-1} \ll \Delta t \ll \Omega_2^{-1}, \quad (12)$$

the driving by  $\Omega_2 \neq 0$  will slowly build up small populations in the other subspaces. These populations, divided by  $\Delta t$ , can then be interpreted as transition rates to the other periods, just as in the one-atom case. We will denote the transition rate from a fluorescence period of type  $i$  to a period of type  $j$  by  $p_{ij}$ . It will turn out that, as expected, the resulting transition rates are insensitive to the particular choice of  $\Delta t$ , as long as Eq. (12) is fulfilled. If the atomic distance is less than three quarters of an optical wave length of the strong transition, the assumption of a three-step telegraph process may no longer be valid, as indicated by the simulations and the remarks at the

end of the last section.

We intend to determine the transition rates  $p_{ij}$  to second order in  $\Omega_2$ . Instead of calculating populations we will determine their changes. This will give an order of  $\Omega_2$  for free. Indeed, a straightforward calculation using Eq. (6) yields the exact relations

$$\begin{aligned} & \frac{d}{dt} \sum_{\text{outer}} \langle \text{outer} | \rho | \text{outer} \rangle \\ &= \Omega_2 \text{Im} \left\{ \sqrt{2} \langle s_{12} | \rho | g \rangle + \langle s_{23} | \rho | s_{13} \rangle + \langle a_{23} | \rho | a_{13} \rangle \right\} \quad (13) \end{aligned}$$

$$\frac{d}{dt} \langle e_2 | \rho | e_2 \rangle = \sqrt{2} \Omega_2 \text{Im} \langle s_{12} | \rho | e_2 \rangle \quad (14)$$

$$\begin{aligned} & \frac{d}{dt} \sum_{\text{inner}} \langle \text{inner} | \rho | \text{inner} \rangle \\ &= - \frac{d}{dt} \left\{ \langle e_2 | \rho | e_2 \rangle + \sum_{\text{outer}} \langle \text{outer} | \rho | \text{outer} \rangle \right\} \quad (15) \end{aligned}$$

where  $|\text{outer}\rangle$  stands for  $|g\rangle$ ,  $|s_{13}\rangle$ ,  $|e_3\rangle$ ,  $|a_{13}\rangle$  and  $|\text{inner}\rangle$  for  $|s_{12}\rangle$ ,  $|a_{12}\rangle$ ,  $|s_{23}\rangle$ ,  $|a_{23}\rangle$ . The various transition rates are then obtained to *second* order in  $\Omega_2$  by inserting the appropriate  $\rho(\Delta t)$  to *first* order in  $\Omega_2$  on the right-hand side of one of these equations.

To obtain the required density matrices to first order in  $\Omega_2$  we write Eq. (6) in the form

$$\dot{\rho} = \mathcal{L}\rho \quad (16)$$

where the Liouvillean  $\mathcal{L} \equiv \mathcal{L}(A_3, \Omega_3, \Delta_2, C_3, \Omega_2)$ , a super-operator, can be read off from Eqs. (6)-(9). One can decompose  $\mathcal{L}$  as

$$\mathcal{L} = \mathcal{L}_0 + \mathcal{L}_{C_3} + \mathcal{L}_{\Omega_2} \quad (17)$$

where

$$\begin{aligned} \mathcal{L}_0 &= \mathcal{L}(A_3, \Omega_3, \Delta_2, 0, 0) \\ \mathcal{L}_{C_3} &= \mathcal{L}(0, 0, 0, C_3, 0) \\ \mathcal{L}_{\Omega_2} &= \mathcal{L}(0, 0, 0, 0, \Omega_2). \end{aligned} \quad (18)$$

$\mathcal{L}_{C_3}$  and  $\mathcal{L}_{\Omega_2}$  are linear in  $C_3$  and  $\Omega_2$ , respectively. We note that  $\mathcal{L}_0$  and  $\mathcal{L}_0 + \mathcal{L}_{C_3}$  can be considered as Liouvillean of Bloch equations and that  $\mathcal{L}_{C_3}$  contains part of the reset operation  $\mathcal{R}$ , while  $\mathcal{L}_{\Omega_2}$  does not. As with usual quantum mechanical perturbation theory in the interaction picture, one has

$$\begin{aligned} e^{\mathcal{L}t} &= e^{(\mathcal{L}_0 + \mathcal{L}_{C_3})t} \\ &+ \int_0^t d\tau e^{(\mathcal{L}_0 + \mathcal{L}_{C_3})\tau} \mathcal{L}_{\Omega_2} e^{(\mathcal{L}_0 + \mathcal{L}_{C_3} + \mathcal{L}_{\Omega_2})(t-\tau)}. \end{aligned} \quad (19)$$

Iteration of this relation gives an expansion of  $e^{\mathcal{L}t}$  in powers of  $\Omega_2$ . We apply this to some state  $\rho_i(0)$  in a subspace corresponding to a fluorescence period of type  $i$ ,  $i = 0, 1, 2$ . First we choose  $t = \delta t$ . Then the first term

on the right-hand side of Eq. (19) gives  $\rho_{ss,i}^{C_3}$ , to high accuracy, while the second is negligible. Since  $\rho_{ss,i}^{C_3}$  is invariant under  $e^{(\mathcal{L}_0 + \mathcal{L}_{C_3})t}$ , developing this further in time to  $t = \Delta t$  gives

$$\rho_i(\Delta t) = \rho_{ss,i}^{C_3} + \int_0^{\Delta t - \delta t} d\tau e^{(\mathcal{L}_0 + \mathcal{L}_{C_3})\tau} \mathcal{L}_{\Omega_2} e^{(\mathcal{L}_0 + \mathcal{L}_{C_3} + \mathcal{L}_{\Omega_2})(\Delta t - \delta t - \tau)} \rho_{ss,i}^{C_3}. \quad (20)$$

To first order in  $\Omega_2$  one therefore has

$$\rho_i(\Delta t) = \rho_{ss,i}^{C_3} + \int_0^{\Delta t - \delta t} d\tau e^{(\mathcal{L}_0 + \mathcal{L}_{C_3})\tau} \mathcal{L}_{\Omega_2} \rho_{ss,i}^{C_3}, \quad (21)$$

where the invariance of  $\rho_{ss,i}^{C_3}$  under  $e^{(\mathcal{L}_0 + \mathcal{L}_{C_3})t}$  has been used again. Now we use the fact that  $\mathcal{L}_0 + \mathcal{L}_{C_3}$ , as a Liouvillean of Bloch equations, has an eigenvalue 0 (corresponding to steady states) and eigenvalues  $\lambda_i$  with  $\text{Re } \lambda_i < 0$ . Here the latter are of the order of  $\Omega_3$  and  $A_3$ . It can be shown that  $\mathcal{L}_{\Omega_2} \rho_{ss,i}^{C_3}$  has no components in the zero-eigenvalue subspace [58]. Therefore, the integrand in Eq. (21) is rapidly damped, and since  $\Delta t - \delta t \gg \Omega_3^{-1}, A_3^{-1}$ , the upper integration limit can be extended to infinity. Therefore we can write

$$\rho_i(\Delta t) = \rho_{ss,i}^{C_3} + \int_0^{\infty} d\tau e^{(\mathcal{L}_0 + \mathcal{L}_{C_3} - \epsilon)\tau} \mathcal{L}_{\Omega_2} \rho_{ss,i}^{C_3} \quad (22)$$

where one takes the limit  $\epsilon \rightarrow +0$  later. Thus we obtain

$$\rho_i(\Delta t) = \rho_{ss,i}^{C_3} + (\epsilon - \mathcal{L}_0 - \mathcal{L}_{C_3})^{-1} \mathcal{L}_{\Omega_2} \rho_{ss,i}^{C_3} + \dots \quad (23)$$

where the limit  $\epsilon \rightarrow +0$  is understood. Thus, to *first order* in  $\Omega_2$ ,  $\rho_i(\Delta t)$  is independent of  $\Delta t$ . Therefore, by Eqs. (13)–(15) the transition rates are, to *second order* in  $\Omega_2$ , independent of the particular choice of  $\Delta t$ , as long as Eq. (12) is satisfied.

We now recall that, for the atomic distances under consideration,  $|C_3|$  is less than  $0.2 A_3$ . Thus,  $\mathcal{L}_{C_3}$  can be considered as a perturbation of  $\mathcal{L}_0$ . By the resolvent expansion one has

$$(\epsilon - \mathcal{L}_0 - \mathcal{L}_{C_3})^{-1} = (\epsilon - \mathcal{L}_0)^{-1} + (\epsilon - \mathcal{L}_0)^{-1} \mathcal{L}_{C_3} (\epsilon - \mathcal{L}_0)^{-1} + \dots \quad (24)$$

and similarly

$$\rho_{ss,i}^{C_3} = \rho_{ss,i}^{(0)} + (\epsilon - \mathcal{L}_0)^{-1} \mathcal{L}_{C_3} \rho_{ss,i}^{(0)} + \dots \quad (25)$$

where  $\rho_{ss,i}^{(0)}$  denotes the limit of  $\rho_{ss,i}^{C_3}$  for  $C_3 \rightarrow 0$ , which is thus a steady state of  $\mathcal{L}_0$ . Inserting this into Eq. (23) gives a joint expansion with respect to  $\Omega_2$  and  $C_3$ ,

$$\begin{aligned} \rho_i(\Delta t) &= \rho_{ss,i}^{C_3} + (\epsilon - \mathcal{L}_0)^{-1} \mathcal{L}_{\Omega_2} \rho_{ss,i}^{(0)} \\ &+ (\epsilon - \mathcal{L}_0)^{-1} \mathcal{L}_{C_3} (\epsilon - \mathcal{L}_0)^{-1} \mathcal{L}_{\Omega_2} \rho_{ss,i}^{(0)} \\ &+ (\epsilon - \mathcal{L}_0)^{-1} \mathcal{L}_{\Omega_2} (\epsilon - \mathcal{L}_0)^{-1} \mathcal{L}_{C_3} \rho_{ss,i}^{(0)} + \dots \end{aligned} \quad (26)$$

for  $i = 0, 1, 2$ . The first term  $\rho_{ss,i}^{C_3}$  does not contribute to the matrix elements for the transition probabilities in Eqs. (13)–(15). For a fluorescence period of type 2 one has

$$\rho_{ss,2}^{(0)} = \rho_{ss}^{(A)} \otimes \rho_{ss}^{(B)} \quad (27)$$

where  $\rho_{ss}^{(A,B)}$  are the steady states of the individual atoms for  $\Omega_2 = 0$  in the 1-3 subspace. For a period of type 1 one has

$$\rho_{ss,1}^{(0)} = \frac{1}{2} \{ \rho_{ss}^{(A)} \otimes |2\rangle\langle 2| + |2\rangle\langle 2| \otimes \rho_{ss}^{(B)} \}, \quad (28)$$

by symmetry. One easily checks that this is annihilated by  $\mathcal{L}_{C_3}$  and therefore  $\rho_{ss,1}^{C_3} = \rho_{ss,1}^{(0)}$  holds for the inner states. For the dark period one obviously has

$$\rho_{ss,0}^{C_3} = |2\rangle\langle 2| \otimes |2\rangle\langle 2| = |e_2\rangle\langle e_2|. \quad (29)$$

One now obtains  $p_{12}$  and  $p_{10}$  to second order in  $\Omega_2$  if one inserts  $\rho_1(\Delta t)$ , to first order in  $\Omega_2$ , for  $\rho$  on the right-hand side of Eqs. (13) and (15), respectively. Similarly, inserting  $\rho_2(\Delta t)$  and  $\rho_0(\Delta t)$ , to first order in  $\Omega_2$ , on the right-hand side of Eq. (15) gives  $p_{21}$  and  $p_{01}$ , respectively, to second order in  $\Omega_2$ . For  $C_3 = 0$ , the familiar transition rates for independent atoms will result.

### A. Transition rates between fluorescence periods of type 0 and type 1

To determine the transition rate  $p_{01}$  from a fluorescence period of type 0 to a period of type 1 we put  $i = 0$  in Eq. (23) and insert it into the right-hand side of Eq. (15). This will yield  $p_{01}$  to second order in  $\Omega_2$  and to all orders in  $C_3$ . By Eq. (9),  $\mathcal{L}_{\Omega_2} |e_2\rangle\langle e_2|$  is a linear combination of states of the form  $|\text{inner}\rangle\langle e_2|$  and  $|e_2\rangle\langle \text{inner}|$ . These are annihilated by  $\mathcal{L}_{C_3}$ , and transformed by  $\mathcal{L}_0$  to states of the same form. Hence, by Eq. (23) and to first order in  $\Omega_2$ ,  $\rho_0(\Delta t)$  is independent of  $C_3$ . Hence  $p_{01}$  is given, to second order in  $\Omega_2$  and to all orders of  $C_3$ , by the expression for two independent atoms, which is twice that of the transition rate for a single atom from a dark to a light period. The latter can be found e.g. in Refs. [38,51]. We have thus obtained, to second order in  $\Omega_2$ ,

$$p_{01} = 2\Omega_2^2 \frac{A_3 \Omega_3^2}{(\Omega_3^2 - 4\Delta_2^2)^2 + 4\Delta_2^2 A_3^2}, \quad (30)$$

which is completely independent of the dipole-dipole interaction. The same argument gives zero for the transition rate from a dark period to a period of type 2.

To obtain the transition rate  $p_{10}$  from a fluorescence period of type 1 to a dark period, we put  $i = 1$  in Eq. (23) and insert it in the right-hand side of Eq. (14). Applying  $\mathcal{L}_{\Omega_2}$  to  $\rho_{ss,1}^{(0)}$  in Eq. (28) gives a linear combination of terms of the form  $|\text{inner}\rangle\langle \text{outer}|$  and  $|\text{inner}\rangle\langle e_2|$ , plus Hermitian conjugates. The former are mapped by

$\mathcal{L}_0 + \mathcal{L}_{C_3}$  into similar terms, while the latter are annihilated by  $\mathcal{L}_{C_3}$ , by Eqs. (7)-(9). Again by Eq. (23), the terms relevant for  $p_{10}$  are independent of  $C_3$ , in view of the matrix elements appearing in Eq. (14). Hence  $p_{10}$  is also given by the corresponding expression for two independent atoms. This is the same as the transition rate for a single atom from a light to a dark period [51]. Hence we find, to second order in  $\Omega_2$  and all orders of  $C_3$ ,

$$p_{10} = \Omega_2^2 \frac{A_3 \Omega_3^2 (A_3^2 + 4\Delta_2^2)}{(A_3^2 + 2\Omega_3^2)[(\Omega_3^2 - 4\Delta_2^2)^2 + 4\Delta_2^2 A_3^2]} . \quad (31)$$

This is again independent of the dipole-dipole interaction.

### B. Transition rates between fluorescence periods of type 1 and type 2

The transition rate  $p_{12}$ , to first order in  $C_3$  and to second order in  $\Omega_2$ , is obtained by inserting  $\rho_1(\Delta t)$  from Eq. (26), for  $i = 1$ , into the right-hand side of Eq. (13). The second term on the right-hand side of Eq. (26) leads to the transition rate for independent atoms. Since  $\mathcal{L}_{C_3} \rho_{ss,1}^{(0)}$  is zero, the last term in Eq. (26) vanishes. The third term can be reduced by some lengthy algebra to the inversion of an  $8 \times 8$  matrix. The inversion is easily performed by

$$p_{21} = \Omega_2^2 \left\{ \frac{2A_3 \Omega_3^2 (A_3^2 + 4\Delta_2^2)}{(\Omega_3^4 - 8\Delta_2^2 \Omega_3^2 + 16\Delta_2^4 + 4A_3^2 \Delta_2^2)(A_3^2 + 2\Omega_3^2)} + \text{Re } C_3(r) \frac{4A_3^2 \Omega_3^2 (A_3^4 \Omega_3^4 + 4A_3^2 \Omega_3^6 - 12A_3^2 \Delta_2^2 \Omega_3^4 - 64A_3^2 \Delta_2^6 - 4A_3^6 \Delta_2^2 - 32A_3^4 \Delta_2^4 - 64\Delta_2^4 \Omega_3^4 + 16\Delta_2^2 \Omega_3^6)}{(A_3^2 + 2\Omega_3^2)^3 (\Omega_3^4 - 8\Delta_2^2 \Omega_3^2 + 4A_3^2 \Delta_2^2 + 16\Delta_2^4)^2} \right\} . \quad (34)$$

This simplifies, for  $\Delta_2 = 0$ , to

$$p_{21} = \Omega_2^2 \left\{ \frac{2A_3^3}{\Omega_3^2 (A_3^2 + 2\Omega_3^2)} + \text{Re } C_3(r) \frac{4A_3^4 (A_3^2 + 4\Omega_3^2)}{\Omega_3^2 (A_3^2 + 2\Omega_3^2)^3} \right\} . \quad (35)$$

*Discussion.* The calculations of  $p_{01}$  and  $p_{10}$  are to second order in  $\Omega_2$  and to all orders in the dipole interaction. For  $p_{12}$  and  $p_{21}$  the calculations are to second order in  $\Omega_2$  and to first order in the dipole interaction, and the results depend only on the real part of  $C_3$ , not on the imaginary part. In the calculation of  $p_{21}$  it turns out that the contributions from the third and fourth term in Eq. (26) individually do depend on  $\text{Im } C_3$ , but in their sum  $\text{Im } C_3$  drops out. If in Eq. (26) one goes to second order in  $C_3$  and inserts this into Eqs. (13) and (15) one obtains  $p_{12}$  and  $p_{21}$  to second order in  $C_3$ . The resulting expressions are not enlightening and therefore not given here, but they do depend on  $\text{Im } C_3$ . Fig. 7 shows how small the second-order dipole-dipole contribution to  $p_{21}$  is for the parameters of the simulations and for distances larger than half a wave length. For smaller distances the results are probably not applicable anyway, as discussed

Maple or Mathematica. It is also possible to calculate the  $81 \times 81$  matrix  $(\epsilon - \mathcal{L}_0)^{-1}$  as well as the relevant matrix elements of the third term by Maple directly. As a result one obtains, to second order in  $\Omega_2$  and to first order in the dipole-dipole interaction,

$$p_{12} = \Omega_2^2 \left\{ \frac{A_3 \Omega_3^2}{\Omega_3^4 - 8\Delta_2^2 \Omega_3^2 + 4A_3^2 \Delta_2^2 + 16\Delta_2^4} + \text{Re } C_3(r) \frac{2A_3^2 \Omega_3^2 (\Omega_3^4 - 4A_3^2 \Delta_2^2 - 16\Delta_2^4)}{(A_3^2 + 2\Omega_3^2)(\Omega_3^4 - 8\Delta_2^2 \Omega_3^2 + 4A_3^2 \Delta_2^2 + 16\Delta_2^4)^2} \right\} . \quad (32)$$

This simplifies, for  $\Delta_2 = 0$ , to

$$p_{12} = \Omega_2^2 \left\{ \frac{A_3}{\Omega_3^2} + \text{Re } C_3(r) \frac{2A_3^2}{\Omega_3^2 (A_3^2 + 2\Omega_3^2)} \right\} . \quad (33)$$

The transition rate  $p_{21}$ , to first order in  $C_3$  and to second order in  $\Omega_2$ , is obtained by inserting  $\rho_2(\Delta t)$  from Eq. (26), for  $i = 2$ , into the right-hand side of Eq. (15). The second term of Eq. (26) leads to the transition rate for independent atoms. Now both the third and fourth term contribute. By some extremely heavy algebra one can reduce the problem to the inversion of a  $16 \times 16$  matrix. Alternatively, one can use the matrix  $(\epsilon - \mathcal{L}_0)^{-1}$  and calculate the relevant matrix elements of Eq. (26) directly by Maple. This yields, to second order in  $\Omega_2$  and to first order in the dipole-dipole interaction,

above.

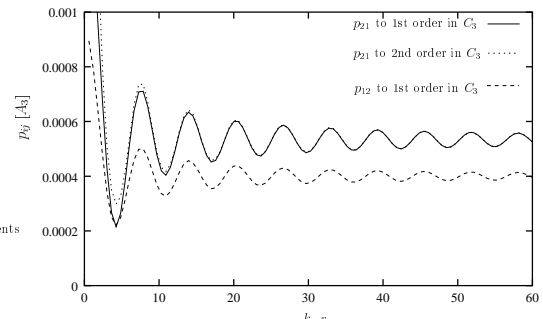


FIG. 7. Transition probabilities  $p_{21}$  to first and second order in  $C_3$  and  $p_{21}$  to first order, for  $\Omega_3 = 0.5A_3$ ,  $\Omega_2 = 0.01A_3$ , zero detuning. The contribution to  $p_{21}$  arising from the second order in  $C_3$  is small.

For  $\Delta_2 = 0$  the coefficients of the  $\text{Re } C_3$  term in Eqs. (33) and (35) are positive. Therefore,  $p_{12}$  and  $p_{21}$  vary with the atomic distance *in phase* with  $\text{Re } C_3$ . For  $\Delta_2 \neq 0$ , however, the coefficients of  $\text{Re } C_3$  in Eqs. (32) and (34) can become negative. Then  $p_{12}$  and  $p_{21}$  vary *opposite* in phase to  $\text{Re } C_3$ .

It will be shown in the next sections that this dependence of  $p_{12}$  and  $p_{21}$  on the detuning of the weak laser entails a corresponding behavior of the double jump rate and an opposite behavior of the mean durations  $T_1$  and  $T_2$ . This opposite behavior of  $T_1$  and  $T_2$  is easy to understand since they are related to the inverse of the transition rates.

## V. DOUBLE JUMPS: COMPARISON WITH THEORY

The results of the last section will now be used to derive an expression for the rate of double jumps. At first the influence of the averaging window  $T_w$  will be neglected. We start from a telegraph process with three steps which correspond to the three fluorescence periods. The process is characterized by the transitions rates  $p_{ij}$  of the last section. A downward double jump within a time interval of length  $\Delta T_{DJ}$  is shown in Fig. 8.

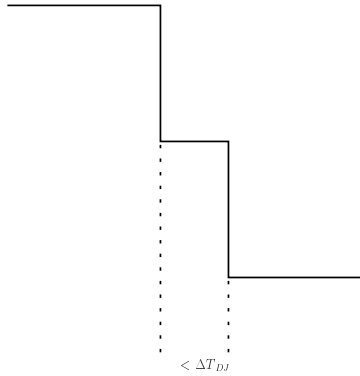


FIG. 8. A downward double jump is a transition from double intensity to single intensity and then to a dark period within a time interval shorter than a prescribed length  $\Delta T_{DJ}$ .

The rate of such downward double jumps is then obtained as follows. For  $i = 0, 1, 2$ , let  $n_i$  be the mean number of periods of type  $i$  per unit time. For a long path of length  $T$  the total number of periods of type  $i$  is then  $N_i(T) = n_i T$ . At the end of each period of type 2 there begins a period of type 1, and the probability for this period of type 1 to be shorter than  $\Delta T_{DJ}$  is given by

$$1 - \exp\{-(p_{10} + p_{12})\Delta T_{DJ}\}.$$

At the end of a period of type 1 the branching ratio for a transition to a period of type 0 is  $p_{10}/(p_{10} + p_{12})$ . Thus during time  $T$  the total number of such downward double jumps, denoted by  $N_{DJ}^{20}(T)$ , is

$$N_{DJ}^{20}(T) = N_2(T) \frac{p_{10}}{(p_{10} + p_{12})} \left\{ 1 - \exp\{-(p_{10} + p_{12})\Delta T_{DJ}\} \right\}$$

and therefore the rate,  $n_{DJ}^{20}$ , of downward double jumps within  $\Delta T_{DJ}$  is

$$n_{DJ}^{20} = n_2 \frac{p_{10}}{(p_{10} + p_{12})} \left\{ 1 - \exp\{-(p_{10} + p_{12})\Delta T_{DJ}\} \right\}. \quad (36)$$

In a similar way one finds that the rate,  $n_{DJ}^{02}$ , of upward double jumps within  $\Delta T_{DJ}$  is

$$n_{DJ}^{02} = n_0 \frac{p_{12}}{(p_{10} + p_{12})} \left\{ 1 - \exp\{-(p_{10} + p_{12})\Delta T_{DJ}\} \right\}. \quad (37)$$

It remains to determine  $n_0$  and  $n_2$ . Since a period of type 1 ends with a transition to a period of either type 0 or type 2 one has, with the respective branching ratios,

$$n_0 = \frac{p_{10}}{p_{10} + p_{12}} n_1 \quad (38)$$

$$n_2 = \frac{p_{12}}{p_{10} + p_{12}} n_1. \quad (39)$$

If one denotes by  $T_i$  the mean durations of a period of type  $i$ , one has

$$\sum_{i=0}^2 n_i T_i = 1. \quad (40)$$

Moreover, one has

$$T_0 = 1/p_{01}, \quad T_1 = 1/(p_{10} + p_{12}), \quad T_2 = 1/p_{21} \quad (41)$$

and this then gives

$$n_0 = \frac{p_{01}p_{21}}{p_{01}p_{21} + p_{21}p_{10} + p_{01}p_{12}} p_{10} \quad (42)$$

$$n_2 = \frac{p_{01}p_{21}}{p_{01}p_{21} + p_{21}p_{10} + p_{01}p_{12}} p_{21}. \quad (43)$$

From this, together with Eqs. (36) and (37), one sees immediately that the rates of upward and downward double jumps are equal,

$$n_{DJ}^{02} = n_{DJ}^{20}. \quad (44)$$

This fact was also observed in the simulations of Section II. The combined number of double jumps therefore equals

$$n_{DJ} \equiv n_{DJ}^{02} + n_{DJ}^{20} = 2 \frac{p_{01}p_{10}p_{12}p_{21}}{(p_{01}p_{21} + p_{21}p_{10} + p_{01}p_{12})(p_{01} + p_{12})} \quad (45)$$

$$\times \left\{ 1 - \exp\{-(p_{10} + p_{12})\Delta T_{DJ}\} \right\}. \quad (46)$$

For  $\Delta T_{DJ} \ll T_1$  and by expanding the exponential, this gives for the combined double jump rate, without correction for the averaging window,

$$n_{DJ} = 2 \frac{p_{01}p_{10}p_{12}p_{21}}{p_{01}p_{21} + p_{21}p_{10} + p_{01}p_{12}} \Delta T_{DJ}. \quad (47)$$

Fig. 9 shows a comparison of this result with the data of the simulation.

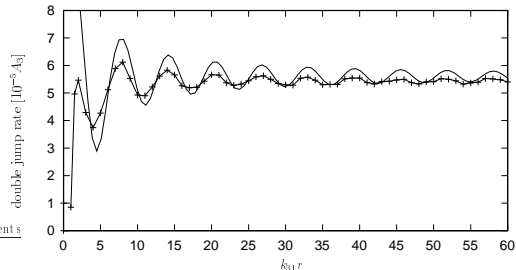


FIG. 9. Double jump rates. Simulation + + +, theory —, uncorrected for averaging window ( $\Omega_3 = 0.5 A_3$ ,  $\Omega_2 = 0.01 A_3$ , zero detuning).

Except for atomic distances less than about three quarters of the wave length of the strong transition the agreement appears as quite reasonable, and the disagreement for small distances is not unexpected since there the intensities start to decrease and a description by a telegraph process may be no longer a good approximation, as pointed out above. But one observes that the theoretical result is systematically above the simulated curve. This minor disagreement, however, is easily explained and can be taken care of as follows. We recall that the simulated data were obtained by averaging the numerical photon emission times with a moving window of length  $\Delta T_w$ . Then, roughly, periods which are shorter than about two thirds of the window length are overlooked, and therefore the number  $n_{2,cor}$  of recorded (or observed) periods of type 2, which enters Eq. (36), is smaller than that given by Eq. (43). The recorded or observed number is, approximately,

$$n_{2,cor} = n_2 \exp\left\{-p_{21} \frac{2}{3} \Delta T_w\right\}, \quad (48)$$

and this expression should be inserted into Eq. (36) for  $n_2$ . In this way one obtains the corrected theoretical curve in Fig. 10.

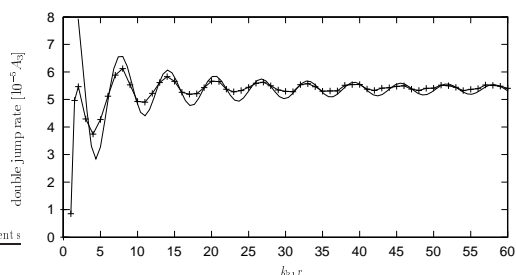


FIG. 10. As in Fig. 9, but theory corrected for averaging window.

The curve changes very little if instead of two thirds one takes 60% or 70% of  $\Delta T_w$ . It is seen that the agreement with the simulated data is much improved for distances greater than three quarters of a wave length of the strong transition.

It still appears, however, that the oscillation amplitudes of the theoretical curve are somewhat larger than those of the simulated curve. This is again understandable as an effect of the averaging procedure. As pointed out in Section II the oscillation amplitudes of the simulated data decrease with the length of the averaging window. If it were possible to choose smaller averaging window the amplitudes should increase, as predicted by the theory.

One can explicitly insert the expressions for  $p_{ij}$  of the last section into Eq. (47), but the result becomes unwieldy. For zero detuning and by expansion of Eq. (47) with respect to  $\text{Re } C_3$  to first order one can show that the coefficient of  $\text{Re } C_3$  is positive. This implies that the double jump rate is *in phase* with  $\text{Re } C_3(r)$  for the atomic distances under consideration and for zero detuning. For increasing detuning the double jump rate can become constant in  $r$  and then change its oscillatory behavior to that of  $-\text{Re } C_3$ . An example for the latter is shown in Fig. 11.

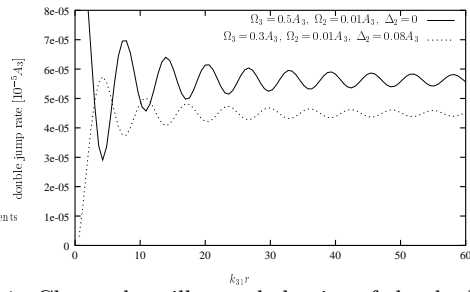


FIG. 11. Changed oscillatory behavior of the double jump rate for increased detuning of the weak driving (uncorrected for averaging window).

## VI. DURATION OF FLUORESCENCE PERIODS: COMPARISON OF THEORY WITH SIMULATION

The mean durations,  $T_0$ ,  $T_1$ , and  $T_2$ , of the three periods were investigated for cooperative effects in Ref. [49] by simulations with averaging windows at discrete times. Here we have performed similar simulations with a moving averaging window. It turns out that both the present and the previous simulation for  $T_i$  are about 15% higher than those predicted by Eq. (41), using the expressions for  $p_{ij}$  of Section IV. This is again due to the use of the averaging window, by which short periods are not recorded. We will now show how this can be taken into account in the theory.

We consider a three-step telegraph process with periods of type 0, 1, and 2, of mean durations  $T_0$ ,  $T_1$ , and  $T_2$ . We assume that periods of length  $\Delta\tau$  or less are not recorded. Fig. 12 shows periods of type 1 which are interrupted by a short period of type 0 and 2, respectively. If the respective short periods are not recorded, then the two periods of type 1 in the left part of the figure are

recorded as a *single* longer period, and similarly for the right part of the figure. This leads to an apparent decrease of shorter periods of type 1 and a corresponding increase of longer periods.

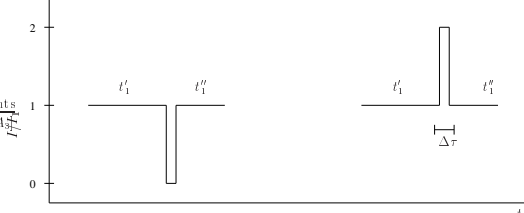


FIG. 12. If periods of length  $\Delta\tau$  or less are overlooked then the distribution of the periods is changed.

To make this quantitative we put  $\lambda_i \equiv 1/T_i$  and denote the number per unit time of periods of type  $i$ , whose duration is less than  $\Delta\tau$ , by  $n_i^{\Delta\tau}$ , i.e.

$$n_i^{\Delta\tau} = n_i \left\{ 1 - \exp\{-\lambda_i \Delta\tau\} \right\}. \quad (49)$$

Per unit time, one has  $n_0^{\Delta\tau}$  occurrences of the situation in the left part of Fig. 12 and  $n_2^{\Delta\tau}$  occurrences of that in the right part. The probability for one of the periods of type 1 in the left or right part of Fig. 12 to have a length lying in the time interval  $(t_1, t_1 + dt_1)$  is  $2\lambda_1 \exp\{-\lambda_1 t_1\} dt_1$ , where the factor of 2 comes from the two possible situations. Therefore, the recorded number, per unit time, of periods of type 1 with duration in  $(t_1, t_1 + dt_1)$  is changed (decreased) by

$$2(n_0^{\Delta\tau} + n_2^{\Delta\tau}) \lambda_1 \exp\{-\lambda_1 t_1\} dt_1 \quad (50)$$

Similarly, the apparent increase of the number, per unit time, of periods of type 1 with duration in  $(t_1, t_1 + dt_1)$  is, by Fig. 12,

$$\begin{aligned} & (n_0^{\Delta\tau} + n_2^{\Delta\tau}) \int \int_{t_1 \leq t'_1 + t''_1 \leq t_1 + dt_1} dt'_1 dt''_1 \\ & \quad \times \lambda_1 \exp\{-\lambda_1 t'_1\} \lambda_1 \exp\{-\lambda_1 t''_1\} \\ & = (n_0^{\Delta\tau} + n_2^{\Delta\tau}) \lambda_1^2 t_1 \exp\{-\lambda_1 t_1\} dt_1. \end{aligned} \quad (51)$$

Denoting by  $\nu_{1\text{rec}}(t_1) dt_1$  the actually recorded number, per unit time, of periods of type 1 with duration in  $(t_1, t_1 + dt_1)$  one obtains from the two previous expressions

$$\begin{aligned} \nu_{1\text{rec}}(t_1) dt_1 &= n_1 \lambda_1 \exp\{-\lambda_1 t_1\} dt_1 \\ &+ (n_0^{\Delta\tau} + n_2^{\Delta\tau}) (\lambda_1^2 t_1 - 2\lambda_1) \exp\{-\lambda_1 t_1\} dt_1. \end{aligned} \quad (52)$$

The average duration of the recorded periods of type 1 will be denoted by  $T_{1,\text{cor}}$ , and it is given by

$$T_{1,\text{cor}} = \int_{\Delta\tau}^{\infty} dt_1 t_1 \nu_{1\text{rec}}(t_1) / \int_{\Delta\tau}^{\infty} dt_1 \nu_{1\text{rec}}(t_1). \quad (53)$$

Using Eq. (52) for  $\nu_{1\text{rec}}(t_1)$  one obtains, after an elementary calculation and for  $\Delta\tau$  satisfying  $\Delta\tau/T_1 \ll 1$ ,

$$T_{1,\text{cor}} = \frac{1}{p_{10} + p_{12}} + \Delta\tau \left\{ 1 + \frac{p_{01}p_{10} + p_{12}p_{21}}{(p_{10} + p_{12})^2} \right\}. \quad (54)$$

The first term is the ideal theoretical value,  $T_1$ , and the remainder is the correction due to non-recorded short periods. In a similar way one obtains

$$T_{0,\text{cor}} = \frac{1}{p_{01}} + \Delta\tau \left\{ 1 + \frac{p_{10}}{p_{01}} \right\} \quad (55)$$

$$T_{2,\text{cor}} = \frac{1}{p_{21}} + \Delta\tau \left\{ 1 + \frac{p_{12}}{p_{21}} \right\} \quad (56)$$

where again the respective first terms are the ideal values,  $T_0$  and  $T_2$ .

To compare this with the simulated data, obtained with a moving averaging window of length  $\Delta T_w = 247 A_3^{-1}$ , we have taken  $\Delta\tau = \frac{2}{3}\Delta T_w$ , as in the previous section, and have plotted the results together with the simulated data in Fig. 13.

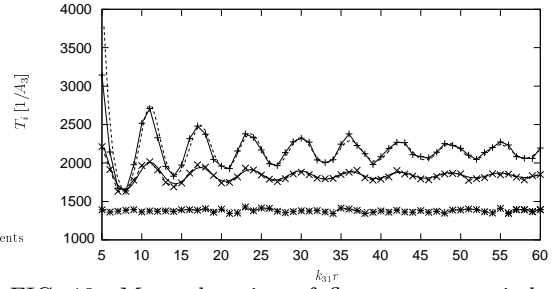


FIG. 13. Mean duration of fluorescence periods. Simulation:  $T_2$   $+++$ ,  $T_1$   $\times \times \times$ ,  $T_0$   $\ast \ast \ast$ . Theory:  $T_2$   $---$ ,  $T_1$   $---$ ,  $T_0$   $....$ , uncorrected for averaging window ( $\Omega_3 = 0.5 A_3$ ,  $\Omega_2 = 0.01 A_3$ , zero detuning).

The agreement is very good. Quite generally, for zero detuning the oscillations of  $T_1$  and  $T_2$  are *opposite* in phase to those of  $\text{Re } C_3(r)$ , as already noted at the end of Section IV. As in the case of the double jump rate,  $T_1$  and  $T_2$  can become constant in  $r$  for particular values of the detuning (different for  $T_1$  and  $T_2$ ), and then change to a behavior *in phase* with  $\text{Re } C_3(r)$ .

The above approach of taking the averaging window into account works for the following reason. For a single atom with macroscopic dark periods it is known that the emission of photons is describable, to high accuracy, by an underlying two-step telegraph process. For two independent atoms with macroscopic dark periods the emissions are therefore described by an underlying three-step telegraph process. For two atoms interacting by a weak dipole-dipole interaction the actual emission process of photons should therefore still have, at least approximately, an underlying three-step telegraph process. What we have done above is replacing the actual emission process by this underlying three-step telegraph process and then incorporating the averaging window by taking into account the influence of the overlooked short periods on the statistics.

## VII. DISCUSSION OF RESULTS

We have investigated cooperative effects in the fluorescence of two dipole-dipole interacting atoms in a  $V$  configuration. One of the excited states of the  $V$  configuration is assumed to be metastable, i.e. with a weak transition to the ground state. When driven by two lasers, a single such configuration exhibits macroscopic dark periods and periods of fixed intensity, like a two-step telegraph process. A system of two such atoms exhibits three fluorescence types, i.e. dark periods and periods of single and double intensity, like a three-step telegraph process. For large atomic distances, when the dipole-dipole interaction is negligible, the total fluorescence just consists of the sum of the individual atomic contributions. For smaller atomic distances the fluorescence may conceivably be modified, and this question has been investigated here, both by simulations and analytically. In particular, we have studied cooperative effects on the rate of double jumps and on the mean duration,  $T_0, T_1$ , and  $T_2$  of the three types of fluorescence periods.

A double jump is a transition from a period of double intensity to a dark period, or vice versa, within a time window of prescribed length. In this paper we have presented simulations for double jump rates which, to our knowledge for the first time, show a marked dependence on the atomic distance. The simulated double jump rates vary in an oscillatory way with the distance and are in phase with  $\text{Re } C_3$ , where  $C_3$  is the complex dipole-dipole coupling constant associated with the strong transitions. The simulations were performed for zero laser detuning. The variation of the double jump rate did not exceed 30 %. We found a similar behavior in simulations of the mean durations,  $T_1$  and  $T_2$ , of the single and double intensity periods, in agreement with simulation results in Ref. [49]. The variation of  $T_2$  was about twice as large as that of  $T_1$ , while  $T_0$  did not depend on the atomic distance.

To check whether or not this behavior is accidental and to allow for arbitrary atomic and laser parameters we have calculated the double jump rate and the mean durations  $T_i$  in closed form analytically. For this we have explicitly determined the transition rates,  $p_{ij}$ , between fluorescence periods of type  $i$  and  $j$  as a function of the atomic distance. When comparing with the simulation results for double jump rates and for  $T_i$  it turns out that one has to take into account the averaging window used for obtaining an intensity curve from the individual photon emissions. With this the agreement between simulation and analytic theory is excellent. In particular, the fact that the simulated double jump rates are *in phase* with  $T_1$  and  $T_2$  *opposite* in phase to  $\text{Re } C_3(r)$  can now be understood from the behavior of the transition rates  $p_{21}$  and  $p_{12}$  which, for the parameters of the simulations, vary as  $\text{Re } C_3(r)$ .

The analytic theory, however, allows also the calculation of double jump rates and mean durations  $T_i$  for

arbitrary atomic and laser parameters, and here there is a surprise. While the simulations were performed for zero laser detuning, the theoretical expressions allow general detuning,  $\Delta_2$ , of the laser which drives the weak transition. It has been shown that for a particular  $\Delta_2$ , which depends on the other parameters, the double jump rate becomes constant and, for larger  $\Delta_2$ , varies opposite in phase to  $\text{Re } C_3(r)$ . A similar change of characteristic behavior also occurs for  $T_1$  and  $T_2$ , for different values of  $\Delta_2$  though. The amplitude of the oscillations with the atomic distance remain in the same region of magnitude as for zero detuning. As pointed out in Ref. [49], a dependence of the oscillations on  $\text{Re } C_3(r)$  is not unexpected since  $\text{Re } C_3(r)$  affects the decay rates of the excited Dicke states of the combined system. But an intuitive argument why the above change of behavior occurs for increased detuning is at present not apparent.

We have pointed out in Section V that there is another statistical property of the fluorescence which can serve as an indicator of the influence of the dipole-dipole interaction and which is probably not too difficult to determine experimentally. This quantity is the rate with which fluorescence periods of definite type occur, in particular the rate of periods with double intensity. Our theoretical results show that this rate behaves similar to the double jump rate, as regards the variation with the atomic distance, and an example is shown in Fig. 14.

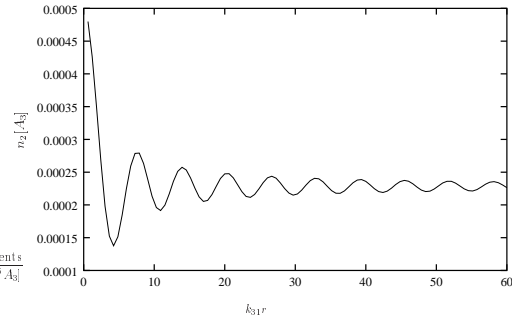


FIG. 14. The theoretical rate,  $n_2$ , of double intensity periods per unit time shows distance-dependent cooperative effects ( $\Omega_3 = 0.5 A_3$ ,  $\Omega_2 = 0.01 A_3$ , zero detuning).

This quantity is probably much easier to measure than the double jump rate or the mean duration  $T_2$ .

Our theoretical approach can be carried over to other level configurations and to more than two atoms. For given parameters the evaluation should be not too difficult. If, however, one is interested in closed algebraic expressions the effort will increase considerably with the number of atoms. In particular, it would be interesting to apply our approach to the situation of the experiment of Ref. [42] with its different level configuration and its three ions in the trap.

[1] G.S. Agarwal, *Quantum Optics*, Springer Tracts in Modern Physics Vol. 70 (Springer-Verlag, Berlin 1974)

[2] G.S. Agarwal, A.C. Brown, L.M. Narducci, and G. Vetrí, Phys. Rev. A **15**, 1613 (1977)

[3] I.R. Senitzki, Phys. Rev. Lett. **40**, 1334 (1978)

[4] H. S. Freedhoff, Phys. Rev. A **19**, 1132 (1979)

[5] G.S. Agarwal, R. Saxena, L.M. Narducci, D.H. Feng, and R. Gilmore, Phys. Rev. A **21**, 257 (1980)

[6] G.S. Agarwal, L.M. Narducci, and E. Apostolidis, Opt. Commun. **36**, 285 (1981)

[7] M. Kus and K. Wodkiewicz, Phys. Rev. A **23**, 853 (1981)

[8] Z. Ficek, R. Tanas and S. Kielich, Opt. Acta **30**, 713 (1983)

[9] Z. Ficek, R. Tanas, and S. Kielich, Phys. Rev. A **29**, 2004 (1984)

[10] Z. Ficek, R. Tanas and S. Kielich, Opt. Acta **33**, 1149 (1986)

[11] J.F. Lam and C. Rand, Phys. Rev. A **35**, 2164 (1987)

[12] Z. Ficek, R. Tanas and S. Kielich, J. Mod. Opt. **35**, 81 (1988)

[13] B.H.W. Hendriks and G. Nienhuis, J. Mod. Opt. **35**, 1331 (1988)

[14] M.S. Kim, F.A.M. Oliveira, and P.L. Knight, Opt. Commun. **70**, 473 (1989)

[15] S.V. Lawande, B.N. Jagatap and Q.V. Lawande, Opt. Commun. **73**, 126 (1989)

[16] Q.V. Lawande, B.N. Jagatap and S.V. Lawande, Phys. Rev. A **42**, 4343 (1990)

[17] Z. Ficek and B.C. Sanders, Phys. Rev. A **41**, 359 (1990)

[18] K. Yamada and P.R. Berman, Phys. Rev. A **41**, 453 (1990)

[19] Th. Richter, Opt. Commun. **80**, 285 (1991)

[20] G. Kurizki, Phys. Rev. A **43**, 2599 (1991)

[21] G.V. Varada and G.S. Agarwal, Phys. Rev. A **45**, 6721 (1992)

[22] D.F.V. James, Phys. Rev. A **47**, 1336 (1993)

[23] R.G. Brewer, Phys. Rev. A **52**, 2965 (1995); Phys. Rev. A **53**, 2903 (1996)

[24] R.G. DeVoe and R.G. Brewer, Phys. Rev. Lett. **76**, 2049 (1996)

[25] P.R. Berman, Phys. Rev. A **50**, 4466 (1997)

[26] T. Rudolph and Z. Ficek, Phys. Rev. A **58**, 748 (1998)

[27] J. von Zanthier, G.S. Agarwal, and H. Walther, Phys. Rev. A **56**, 2242 (1997)

[28] Ho Trung Dung and Kikuo Ujihara, Phys. Rev. Letters **84**, 254 (2000)

[29] B.A. Grishanin and V.N. Zadkov, Laser Phys. **8**, 1074 (1998)

[30] A. Beige and G.C. Hegerfeldt, Phys. Rev. A **58**, 4133 (1998)

[31] Ch. Skornia, J. von Zanthier, E. Werner and H. Walther (unpublished)

[32] Th. Sauter, R. Blatt, W. Neuhauser, and P.E. Toschek, Phys. Rev. Lett. **57**, 1697 (1986)

[33] W. Nagourney, J. Sandburg, and H. Dehmelt, Phys. Rev. Lett. **56**, 2797 (1986)

[34] J.C. Bergquist, R.G. Hulet, W.M. Itano, and D.J. Wineland, Phys. Rev. Lett. **57**, 1699 (1986)

[35] W.M. Itano, J.C. Bergquist, R.G. Hulet, and D.J. Wineland, Phys. Rev. Lett. **59**, 2732 (1987)

[36] H.G. Dehmelt, Bull. Am. Phys. Soc. **20**, 60 (1975)

[37] R.J. Cook and H.J. Kimble, Phys. Rev. Lett. **54**, 1023 (1985); H.J. Kimble, R.J. Cook, and A.L. Wells, Phys. Rev. A **34**, 3190 (1986)

[38] C. Cohen-Tannoudji and J. Dalibard, Europhys. Lett. **1**, 441 (1986)

[39] G. Nienhuis, Phys. Rev. A **35**, 4639 (1987); M. Porrati and S. Putterman, Phys. Rev. A **39**, 3010 (1989); S. Reynaud, J. Dalibard and C. Cohen-Tannoudji, IEEE Journal of Quantum Electronics **24**, 1395 (1988); A. Schenzle und R.G. Brewer, Phys. Rev. A **34**, 3127 (1986)

[40] A. Beige and G.C. Hegerfeldt, J. Phys. A **30**, 1323 (1997)

[41] For dark periods without a metastable state see G.C. Hegerfeldt and M.B. Plenio, Phys. Rev. A **46**, 373 (1992)

[42] Th. Sauter, R. Blatt, W. Neuhauser and P.E. Toschek, Opt. Commun. **60**, 287 (1986)

[43] M. Lewenstein and J. Javanainen, Phys. Rev. Lett. **59**, 1289 (1987), IEEE J. Quantum Electron. **24**, 1403 (1988)

[44] G.S. Agarwal, S.V. Lawande and R. D'Souza, IEEE J. Quantum Electron. **24**, 1413 (1988)

[45] S.V. Lawande, Q.V. Lawande and B.N. Jagatap, Phys. Rev. A **40**, 3434 (1989)

[46] Chung-rong Fu and Chang-de Gong, Phys. Rev. A **45**, 5095 (1992)

[47] W.M. Itano, J.C. Bergquist, and J.C. Wineland, Phys. Rev. A **38**, 559 (1988)

[48] R.C. Thompson, D.J. Bates, K. Dholakia, D.M. Segal, and D.C. Wilson, Phys. Scr. **46**, 285 (1992)

[49] A. Beige and G.C. Hegerfeldt, Phys. Rev. A **59**, 2385 (1999)

[50] G.C. Hegerfeldt and T.S. Wilser, in: *Classical and Quantum Systems*. Proceedings of the Second International Wigner Symposium, July 1991, edited by H.D. Doebner, W.Scherer, and F. Schroeck, World Scientific (Singapore 1992), p. 104

[51] T.S. Wilser, Doctoral Dissertation, University of Göttingen (1991)

[52] G.C. Hegerfeldt, Phys. Rev. A **47**, 449 (1993)

[53] G.C. Hegerfeldt and D.G. Sondermann, Quantum Semiclass. Opt. **8**, 121 (1996)

[54] For a recent review see M. B. Plenio and P.L. Knight, Rev. Mod. Phys. **70**, 101 (1998)

[55] A. Beige and G.C. Hegerfeldt, Phys. Rev. A **53**, 53 (1996)

[56] A. Beige, G.C. Hegerfeldt, and D.G. Sondermann, Quantum Semiclass. Opt. **8**, 999 (1996)

[57] W.H. Press, B.P. Flannery, S.A. Teukolsky and W. Vetterling, *Numerical Recipes*, (Cambridge University Press, Cambridge 1986)

[58] If  $\mathcal{L}_{\Omega_2} \rho_{ss}^{C_3}$  had a zero-eigenvalue component this would show up as a divergence when  $\epsilon \rightarrow 0$  in Eq. (22), leading to a term proportional to  $\Delta t - \delta t$  in Eq. (21). It will be seen later that this does not happen.